

Global flow waves in chemically induced convection

Kai Matthiessen and Stefan C. Müller

Max-Planck-Institut für molekulare Physiologie, Rheinlanddamm 201, 44139 Dortmund, Germany

(Received 20 January 1995)

The spatial distribution of the oscillatory flow in convection driven by chemical waves is visualized by a method that uses the differences in light transmission caused by the tilt of the wave fronts. The images show large flow waves with a wavelength on the order of ten chemical wavelengths traveling through the dish towards the center of the underlying spiral wave.

PACS number(s): 47.70.Fw, 47.20.Bp, 47.20.Dr, 82.20.Mj

INTRODUCTION

The Belousov-Zhabotinsky (BZ) reaction is a well known example of a pattern forming system evolving far from equilibrium. When using the appropriate chemical recipes the solution remains in an excitable state [1]. One can induce circular waves by locally exciting the solution with a silver wire. Breaking of wave fronts leads to spiral waves. This behavior is experimentally and theoretically well examined [2,3].

In many studies of recent years the chemical waves are investigated in a thin layer of gel to avoid hydrodynamic disturbances. On the other hand, the coupling between chemical wave propagation and hydrodynamic flow in the liquid solution is of great interest in itself. Several authors have studied the appearance of convection in a thin layer of an excitable BZ solution in a covered or uncovered Petri dish with an open liquid-gas interface [4–11]. In an uncovered dish Marangoni-type convection predominates due to evaporative cooling of the surface. This flow leads *inter alia* to the so-called mosaic patterns, stationary structures induced by hydrodynamic flow [5–7].

In the covered dish these effects are suppressed. Here one can observe hydrodynamic flow in the reaction solution that is directly induced by the propagating chemical waves [8]. As possible mechanisms for this coupling between waves and convection, gradients in density or surface tension are considered [9]. These gradients may be caused by the process heat as well as by the chemical composition of the medium. The chemically induced flow is measured locally by observing suspended small particles under a microscope. Its behavior depends on the chemical wavelength. The so-called discrete flow occurs in a system with circular waves characterized by a large wavelength (≥ 5 mm). Each wave front carries a pair of vortices through the solution [10,11]. In spiral waves, which propagate with a shorter wavelength of the order of 1 mm, the flow behavior is more complicated. In this case transitions between different flow regimes take place during the evolution of the spiral wave. After an induction period, where the flow does not differ from the case of circular waves, the behavior changes to a unidirectional flow lasting for about 15–20 min. Then there occurs a strong oscillatory flow that changes its direction

once with every passing wave front [11].

In this work we provide direct evidence that this flow spreads over much more than one single wave front. Already in former publications [8,11,12] arguments were put forward that the oscillatory flow is a global phenomenon. The reason for this conjecture was the observation of a simultaneous tilt of three or four wave fronts near the measuring point. The moving solution deforms the wave fronts so that they look less sharp in the transmitted light. The simultaneously appearing flattening of several neighboring fronts is a hint that a single flow cell reaches over more than just one discrete front.

We present a method that also makes use of this front deformation due to the hydrodynamic motion of the solution. In addition to the microscope camera for the local flow measurement a second camera is introduced for the global view. The video images are analyzed with image processing routines to visualize the tilted fronts in the whole dish. The resulting images show global flow waves with a wavelength on the order of about ten chemical waves traveling through the dish towards the spiral center.

EXPERIMENTAL SETUP

All experiments are carried out in a quite reactive BZ solution which remains excitable for about 45 min. The initial concentrations of the components are as follows (as in [8]): 340 mM NaBrO₃, 48 mM NaBr, 95 mM malonic acid, 378 mM H₂SO₄, and 3.5 mM ferroin as catalyst and indicator. Four ml of the solution are filled in a Petri dish with a diameter of about 7 cm. By cleaning the dish very carefully it is possible to avoid any nucleation centers for CO₂ bubbles so that all the gas produced during the reaction has to diffuse through the surface. In addition, the cleaning procedure suppresses wave generation at the dish boundaries. A silver wire induces a chemical wave if it is dipped into the solution. Breaking up this front with an air stream from a pipette leads to a pair of spiral waves [13]. To detect hydrodynamic flow small latex particles with a diameter of 0.5 μ m are added at a concentration low enough that the reaction is not influenced. These particles serve as scattering centers for light from a laser beam which passes the dish at an angle of about 45° (Fig. 1). To detect the particles a small sec-

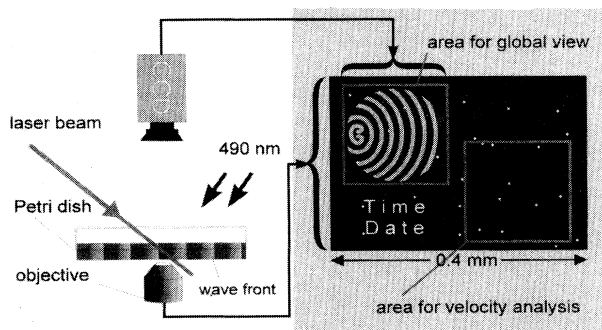


FIG. 1. Experimental setup: Petri dish observed by two cameras (left side); the electronic image overlay of the two camera outputs (right side).

tor of the liquid is observed through an inverse microscope (Zeiss IM35) by a vidicon camera with a contrast amplifying unit (Hamamatsu C2400). The optical setup depicts an area of the Petri dish with a side length of about 0.4 mm on the video screen. By changing the focal plane one can distinguish about 30 layers of the solution, i.e., with a resolution of about $25 \mu\text{m}$. The image shows the latex particles as several bright moving spots in front of a dark background. The velocity of these particles represents the local flow velocity.

Due to the large magnification the camera shows only a small sector of the reaction vessel. In order to correlate the observed flow with chemical wave phenomena it is important to have also a global view of the Petri dish, where chemical wave fronts can be observed at maximum contrast. For this purpose the dish is illuminated by blue light (490 nm, at the highest difference of absorption between ferroin and ferriin) from above in a slightly tilted angle and watched with a CCD camera (Hamamatsu C3077). To store the information of both cameras simultaneously, the images from this camera are fixed electronically into the microscope images where they fill one quarter of the screen (right side of Fig. 1). The resulting sequence of images is recorded on videotape with a time lapse recorder.

For further examination the images are digitized on a personal computer with a frame grabber card (with this setup the smallest delay between two frames is 280 ms). By choosing different areas of the stored images it is possible to digitize the floating particles and the global view separately. The local flow velocity is calculated automatically using the spatial filtering method [14,15]. For this method each image is modulated with a one-dimensional sinus and then integrated to one value. As the bright spots pass minima and maxima of the sinus the integral value will rise and fall. The frequency of these changes is proportional to the velocity of the moving particles. Due to the one-dimensional sinus modulation this method can only analyze flow in one direction. To get vectors one has to estimate the x and y directions separately and superpose them. Since the second dimension is not used for the calculation we can integrate the images already during the digitization in one dimension and reduce the data by a factor of about 100. Each frame is stored as only one line. Thus it is possible to calculate flow from a large

amount of typically 8000 frames.

For the analysis of the global view small changes in the local intensity are visualized by background subtraction, smoothing by a moving average over 15 pixels and contrast enhancement. These image processing procedures are implemented on a workstation using the interactive data language (IDL) program packet (Research Systems Inc. Version 2.2).

RESULTS

Figure 2 shows the flow evolution as measured on the surface of the liquid layer in the Petri dish after the creation of a pair of spirals. In this case the spiral center lies about 1 cm away from the boundary while the examination area is located in the middle of the dish. The observed flow can be divided into three phases. First there appears a discrete flow similar to the behavior in a system with circular waves [11]. During the evolution of the spiral wave the fronts move closer together. As a result the hydrodynamic flow changes first to a unidirectional regime, i.e., the flow direction does not change any more and the flow velocity is low. After about 20 min a strong flow occurs that changes its direction approximately once with every passing wave front. The amplitude of this flow has a maximum at the surface, disappears at middle height of the layer, and is more than three times less near the bottom. In the measurement shown in the figure the flow is rather irregular, but also more regular oscillations are observed, as documented in [11]. These oscillations are the object of the following investigations.

Although the locally observed oscillatory flow behavior does not obviously allow us to reconstruct the hydrodynamics for the whole dish, this flow was already assumed to be global in former publications as a big convection cell should fill a large portion of the dish [11]. Apart from this it has always been an open question how this flow fits into the circular geometry of the Petri dish. To fill the gap between local flow measurement and global system properties we now apply digital image processing procedures to the images obtained from the global view in the experimental setup of Fig. 1.

As indicated above, the flow induces a deformation of the wave fronts as it tilts the front from the vertical direc-

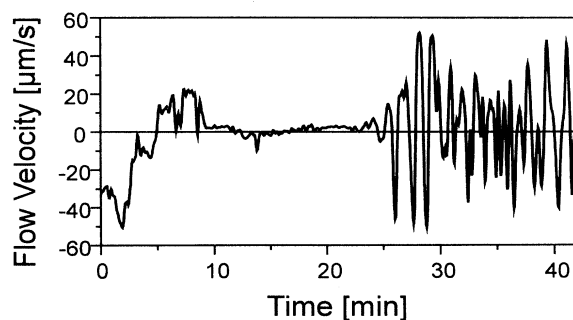


FIG. 2. Temporal evolution of the flow velocity at the top of the Belousov-Zhabotinsky solution layer in the center of the Petri dish after inducing a pair of spirals near the boundary.

tion. Figure 3 shows the deformed wave profiles where graph (a) represents the profiles with a surface flow against and graph (b) in the direction of wave propagation. Curve (c) shows a time series of integrals over subsequent curves like (a) and (b). The positions of profiles (a) and (b) are marked in the diagram. The integral values are higher in the case with flow in the direction of wave propagation. The flow leads to changes of about 5–10% in the local light transmission. These small differences can be visualized in the global view image by different image processing procedures. First the background is subtracted to suppress inhomogeneities in illumination. Then the images are smoothed to remove the structure of the single wave fronts. Afterwards the contrast is amplified and pseudocolors may be added.

The result of these procedures is shown in Fig. 4. The nine images are snapshots of the Petri dish equidistant in time. The time interval between them amounts to 8.4 s. The spots on the dish area are smoothed latex particles from the local view which appear in the overlay of the image (see Fig. 1). On image (b) one can see a bright band appearing in the left third of the dish, representing surface flow in the direction of wave propagation. In the course of time this band gets broader and moves to the right side towards the center of the spiral wave where it disappears. This behavior corresponds to a wave of global flow that travels through the dish.

Figure 5 shows a similar scenario for conditions where rotational symmetry is given by placing the spiral centers in the middle of the dish. On the first image the measuring point for the local view can be seen near the right

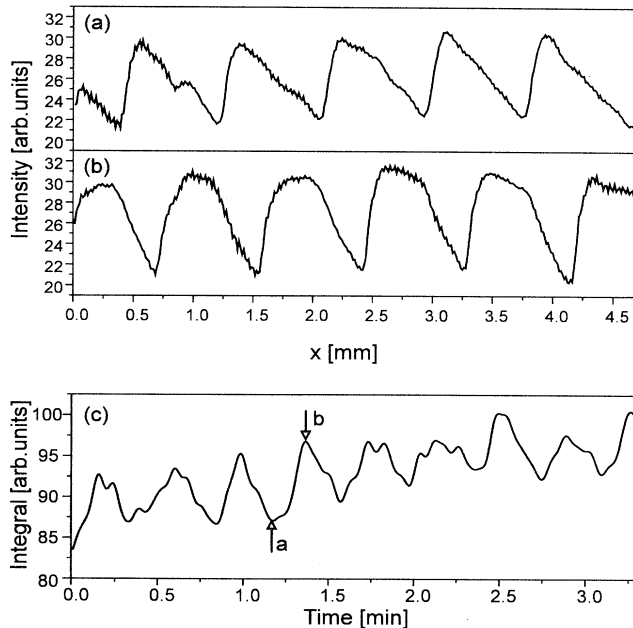


FIG. 3. Deformation of wave profiles by hydrodynamic flow; profile with surface flow against (a) and in the direction of (b) wave propagation. The setup for these measurements is shown in Ref. [12]. (c) is a sequence of curves like (a) and (b), each integrated in x direction.

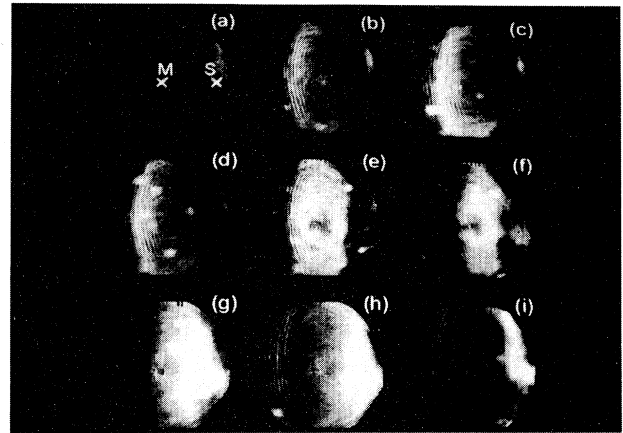


FIG. 4. Global view of the oscillatory flow in a system with the spiral center (S) near the right boundary. The images are treated by background subtraction, smoothing, and contrast enhancement. The time delay between the frames is 8.4 s. The point of flow measurement is located in (M).

boundary. As in the first measurement (Fig. 4), the bright band appears in the second image with a circular geometry near the dish boundary. It also moves towards the spiral center as time proceeds and finally disappears.

It remains to show how the propagation of the bright bands in the global view and the occurring hydrodynamic flow are connected with each other. For this purpose the local light transmission is directly compared with the local flow velocity in Fig. 6. The flow curve (a) in part I of the figure is the portion of the curve in Fig. 2 measured between 24.5 and 33.7 min. For the transmission curve

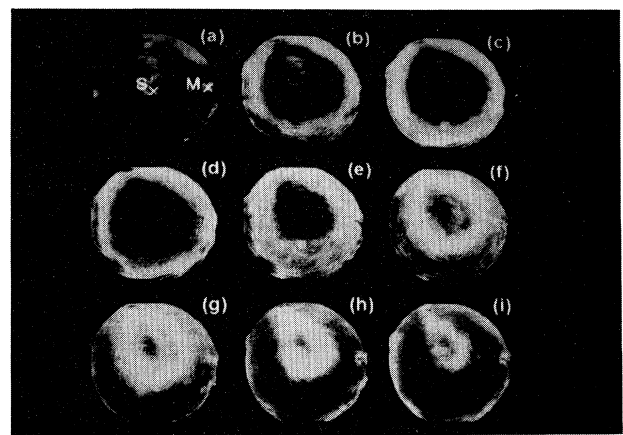


FIG. 5. Global view of the oscillatory flow in a system with the spiral center (S) in the middle of the dish. The conditions are the same as for Fig. 4. The point of flow measurement is located in (M).

(b) a long film with images like those in Fig. 4 was recorded and the average intensity was determined in a small area of 20×20 pixels next to the measuring point. This curve represents the local transmitted light intensity in the point of flow measurement. A superposed positive drift of the transmitted light intensity is due to the aging of the system.

A comparison of these curves shows that both have the same periodicity. Due to the rather irregular form of the oscillatory flow in this experiment as mentioned above the peaks of each oscillation have different characteristic shapes. With regard to these shapes there is also a clear correlation between the flow curve and the curve of transmitted light. In Fig. 6 (II) the corresponding curves for the rotational symmetric case are presented. The similar shape of both curves is again obvious.

DISCUSSION AND CONCLUDING REMARKS

The close correlation between the different curves in Fig. 6 proves the connection between flow phenomena and the observed bright bands in chemically driven convection. Since there is a correspondence between the periodicity of the two curves and between the form of the single peaks one can conclude that the bright bands visualize the local flow state of the system. Even the small positive phase shift between flow and illumination is easily explained, since the tilt of a wave front is a reaction to the hydrodynamic motion and follows the flow with a certain time delay.

The optical measurements provide a tool for detecting the global aspect of the convection in the dish, whereas our method for direct flow measurement allows only estimations in a small area. From the global view one can see that the strong flow that appears after 15 to 20 min in a system with spiral wave propagation is a global phenomenon. As the bright bands show regions with simultaneously tilted wave fronts we observe a large global flow wave traveling through the dish towards the spiral center. The flow has a wavelength that is more than ten times longer than the chemical wavelength and is always tangential to the chemical wave front.

These measurements present a first step towards the analysis of the global aspects of this flow. For further examinations it would be very useful to develop a method

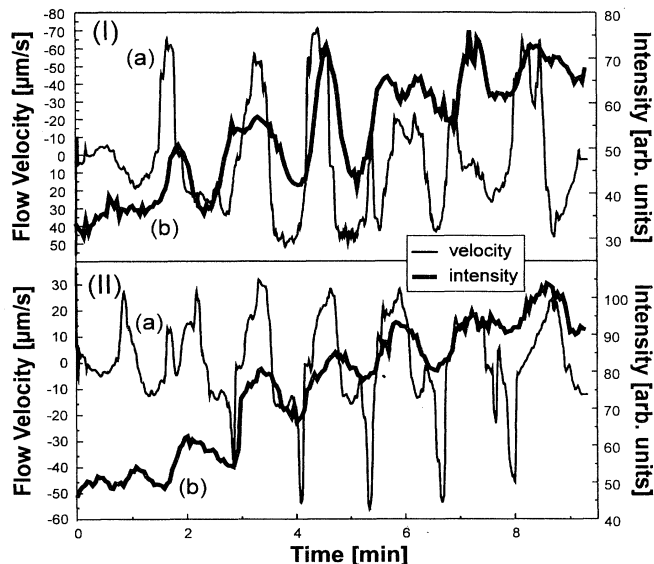


FIG. 6. Comparison between local light transmission and flow for the spiral center near the boundary (I) and in the middle (II) of the dish. Curves (a) depict the flow velocity estimated with the spatial filtering program, curves (b) show the local intensity of transmitted light near the point of flow measurement.

for direct simultaneous flow measurement at several points in the reaction layer.

Other experiments are necessary and underway to clarify the mechanism of the coupling between hydrodynamics and chemical wave propagation. Possible driving forces are gradients in the local density or surface tension induced by differences in temperature or in the composition of the solution. Consequently the exact temperature difference between the oxidized and the reduced state in the waves should be evaluated. Also the time dependence of the surface tension has to be measured very carefully since the gradients are very small.

ACKNOWLEDGMENT

This work was supported by the Deutsche Forschungsgemeinschaft.

- [1] A. M. Zhabotinsky and A. N. Zaikin, *Nature (London)* **225**, 535 (1970).
- [2] J. J. Tyson and J. P. Keener, *Physica D* **32**, 327 (1988).
- [3] *Oscillations and Traveling Waves in Chemical Systems*, edited by R. J. Field and M. Burger (Wiley, New York, 1971).
- [4] Martin Diewald and Helmut R. Brand, *Chem. Phys. Lett.* **216**, 566 (1993).
- [5] M. Orbán, *J. Am. Chem. Soc.* **102**, 4311 (1980).
- [6] K. I. Agladze, V. I. Krinsky, and A. M. Pertsov, *Nature (London)* **308**, 834 (1984).
- [7] S. C. Müller, Th. Plesser, and B. Hess, *Ber. Bunsenges. Phys. Chem.* **89**, 654 (1985).
- [8] H. Miike, S. C. Müller, and B. Hess, *Chem. Phys. Lett.* **144**, 515 (1988).
- [9] J. A. Pojman and I. R. Epstein, *J. Phys. Chem.* **94**, 4966 (1990).
- [10] Th. Plesser, H. Wilke, and K. H. Winters, *Chem. Phys. Lett.* **200**, 158 (1992).
- [11] H. Miike, S. C. Müller, and B. Hess, *Phys. Lett. A* **141**, 25 (1989).
- [12] H. Miike and S. C. Müller, *Chaos* **3**, 21 (1993).
- [13] S. C. Müller, Th. Plesser, and B. Hess, *Science* **230**, 661 (1985).
- [14] Y. Aizu and T. Asakura, *Appl. Phys. B* **43**, 209 (1987).
- [15] H. Miike, H. Yamamoto, M. Momota, and H. Hashimoto, in *Pattern Formation in Complex Dissipative Systems*, edited by S. Kai (World Scientific, Singapore, 1992), pp. 191–200.

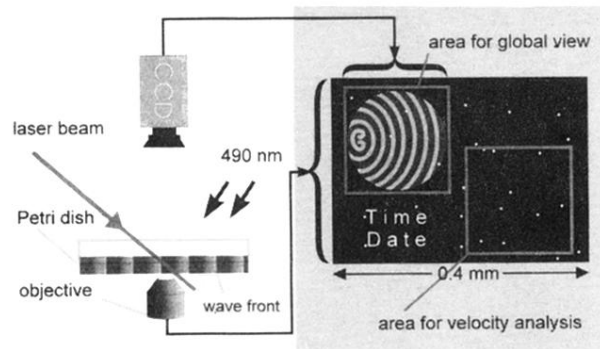


FIG. 1. Experimental setup: Petri dish observed by two cameras (left side); the electronic image overlay of the two camera outputs (right side).

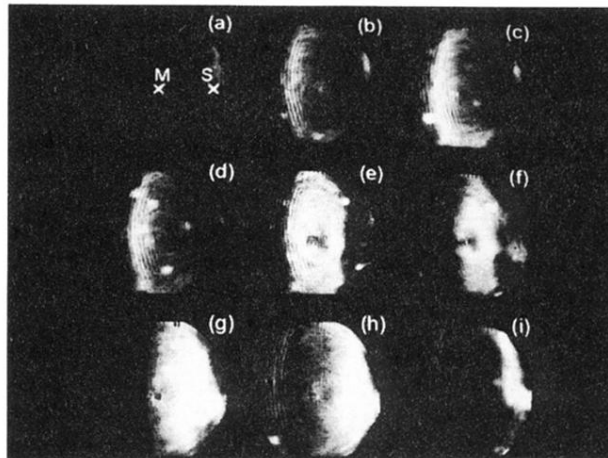


FIG. 4. Global view of the oscillatory flow in a system with the spiral center (S) near the right boundary. The images are treated by background subtraction, smoothing, and contrast enhancement. The time delay between the frames is 8.4 s. The point of flow measurement is located in (M).

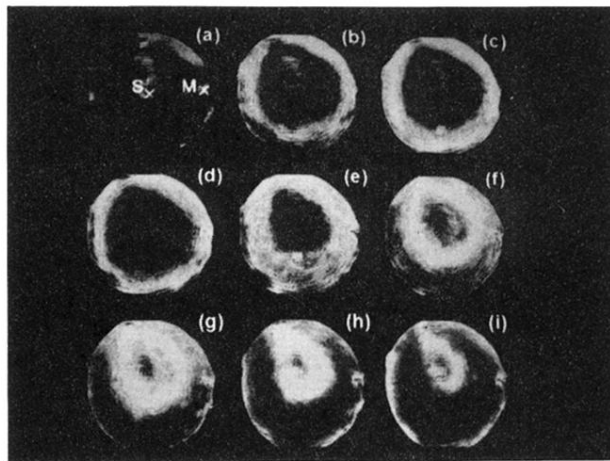


FIG. 5. Global view of the oscillatory flow in a system with the spiral center (S) in the middle of the dish. The conditions are the same as for Fig. 4. The point of flow measurement is located in (M).